Chemical, experimental, and morphological evidence for diagenetically altered melanin in exceptionally preserved fossils

Caitlin Colleary[a,b], Andrei Dolocan[c], James Gardner[d], Suresh Singh[a], Michael Wuttke[e], Renate Rabenstein[f], Jörg Habersetzer[f], Stephan Schaal[f], Mulugeta Feseha[g], Matthew Clemens[h], Bonnie F. Jacobs[h], Ellen D. Currano[i], Louis L. Jacobs[h], Rene Lyng Sylvestersen[j], Sarah E. Gabbott[k], and Jakob Vinther[a,d,l,1]

[a]School of Earth Sciences, University of Bristol, Bristol BS8 1RJ, United Kingdom; [b]Department of Geosciences, Virginia Polytechnic Institute and State University, Blacksburg, VA 24060; [c]Texas Materials Institute, University of Texas at Austin, Austin, TX 78712; [d]Jackson School of Geosciences, University of Texas at Austin, Austin, TX 78712; [e]Department for the Conservation of the Cultural Heritage of Rhineland-Palatinate, 55116 Mainz, Germany; [f]Department of Palaeoanthropology and Messel Research, Senckenberg Research Institute, 60325 Frankfurt am Main, Germany; [g]Paleoanthropology and Paleoenvironment Program, School of Earth Sciences, College of Natural Sciences, Addis Ababa University, Addis Ababa, Ethiopia; [h]Roy M. Huffington Department of Earth Sciences, Southern Methodist University, Dallas, TX 75275; [i]Departments of Botany and Geology & Geophysics, University of Wyoming, Laramie, WY 82071; [j]Division of Natural History, Muse®um, 7800 Skive, Denmark; [k]Department of Geology, University of Leicester, Leicester LE1 7RH, United Kingdom; and [l]School of Biological Sciences, University of Bristol, Bristol BS8 1TQ, United Kingdom

In living organisms, color patterns, behavior, and ecology are closely linked. Thus, detection of fossil pigments may permit inferences about important aspects of ancient animal ecology and evolution. Melanin-bearing melanosomes were suggested to preserve as organic residues in exceptionally preserved fossils, retaining distinct morphology that is associated with aspects of original color patterns. Nevertheless, these oblong and spherical structures have also been identified as fossilized bacteria. To date, chemical studies have not directly considered the effects of diagenesis on melanin preservation, and how this may influence its identification. Here we use time-of-flight secondary ion mass spectrometry to identify and chemically characterize melanin in a diverse sample of previously unstudied extant and fossil taxa, including fossils with notably different diagenetic histories and geologic ages. We document signatures consistent with melanin preservation in fossils ranging from feathers, to mammals, to amphibians. Using principal component analyses, we characterize putative mixtures of eumelanin and phaeomelanin in both fossil and extant samples. Surprisingly, both extant and fossil amphibians generally exhibit melanosomes with a mixed eumelanin/phaeomelanin composition rather than pure eumelanin, as assumed previously. We argue that experimental maturation of modern melanin samples replicates diagenetic chemical alteration of melanin observed in fossils. This refutes the hypothesis that such fossil microbodies could be bacteria, and demonstrates that melanin is widely responsible for the organic soft tissue outlines in vertebrates found at exceptional fossil localities, thus allowing for the reconstruction of certain aspects of original pigment patterns.

paleocolor | melanosome | mass spectrometry | diagenesis | pigmentation

Since melanosomes were first described in fossil feathers (1), a number of studies have made inferences about original colors of extinct vertebrates, which were based on structural and molecular analyses (2–8). However, these interpretations have been questioned (9–11). Animals synthesize two chemically distinct types of melanin: eumelanin (black to dark brown in color) and phaeomelanin (rufous, brown, and buff in color), occurring in eumelanosomes and phaeomelanosomes, respectively. Melanin is an extremely recalcitrant, complexly cross-linked polymer, which is mainly known to degrade through oxidation (12). The nature and function of eumelanin in organisms has been suggested as a possible explanation for its high preservation potential (1). In extant mammals and birds, eumelanosomes are oblong, with a higher aspect ratio than phaeomelanosomes, which are smaller and more spherical (3, 13). It is not clear whether other amniotes or fishes produce morphologically distinct melanosomes, but chemical

evidence distinguishes pure eumelanin and phaeomelanin in turtles (14), and phaeomelanin has been tentatively reported in frogs (15), fish (16), and chitons (Mollusca) (17). Melanosome morphology currently serves as the primary basis for interpretations of fossil feather color, as it correlates with several distinct melanin-based colors and iridescence in modern birds (1, 3, 4). However, maturation experiments simulating diagenesis in recent feathers suggest that the dimensions of melanosomes are altered when subjected to high pressures and temperatures (5, 18), suggesting that melanosome morphology may not be a reliable indicator of color in fossil feathers (19). Further, outside of mammals and birds (13), the extent to which melanosome morphology is a reliable indicator of melanin chemistry, and therefore color, is unknown.

Recent postulations have suggested that oblong and spheroidal microstructures preserved in carbonaceous films are of bacterial origin rather than fossilized melanosomes (10). It was argued that bacteria cultured on modern feathers do not appear to differ in gross morphology from melanosomes (10). However, Moyer et al. (10) failed to factor in the arrangement and size of the observed bacteria, which were several times larger than the

---

Significance

Melanin is a widespread pigment that provides black to reddish brown hues to organisms. Recent evidence has shown that melanin is retained in exceptionally preserved fossils, including feathered dinosaurs, allowing the reconstruction of ancient color patterns. However, little is known about the chemical preservation of melanin or its distribution in the fossil record. Here, we show that melanin is preserved in a number of soft-bodied fossils, but its burial under high pressure and temperature for millions of years alters its original chemistry. The widespread occurrence of melanin substantiates the applicability of reconstructing aspects of original color patterns and allows us to dismiss the alternative suggestion that these structures are microbial in origin.

---

melanosomes recorded in any known vertebrate integument and do not exhibit the unique arrangement or alignment that melanosomes display in feathers (20). Bacterial remains—including microbial mats (21)—occur throughout the fossil record from the Archean to the present (22). These may be preserved via a number of taphonomic pathways, e.g., phosphatization (23) or silicification (24), but are not confidently known to be preserved as solid carbonaceous bodies similar to melanosomes.

Analytical techniques that detect biomolecules indicate that melanin granules occur in fossil cephalopods (25) and that melanin-bearing melanosomes are preserved in fossil fish (7, 26) and marine reptiles (8). The most conclusive and comprehensive chemical study to date shows the presence of chemically intact melanin in quantities of ~10% in Jurassic cephalopod ink sacs (25, 27). Other studies have demonstrated the applicability of time-of-flight secondary ion mass spectrometry (TOF-SIMS), a surface-sensitive technique, which collects in situ mass spectrometric data from fossil samples with only minor alteration of the sample surface (7, 8, 28). The secondary ion spectra of putative fossil melanosomes contain the representative markers that are found in extant melanin samples qualitatively (7, 8), and are distinct from the spectra acquired on bacterial samples and on aromatic organic molecules similar to melanin, such as porphyrins (7, 8). However, when quantified using principal component analysis (PCA), the fossil and extant melanin samples are also distinct (8), indicating that they consist of molecules of different composition, phase, or structure.

We hypothesize that fossil melanosomes contain diagenetically altered melanin and explore the chemical composition of fossil melanosomes by analyzing pure samples of extant melanin and previously unstudied vertebrate fossils using TOF-SIMS. To test our hypothesis, we performed maturation experiments of melanin. We subjected pure melanin extracts to high pressure and temperatures (200 °C/250 bar and 250 °C/250 bar, respectively, for

24 h) in sealed gold tubes to mimic burial conditions and the resulting chemical alterations (29, 30). We compare the TOF-SIMS spectra of fresh, artificially matured, and fossil samples by PCA. We chose a diverse and complementary array of fossils, with soft tissue preservation and discernible melanosomes, from a wide range of localities to understand the significance of diagenesis and taxonomy in fossil melanin composition.

Results

Melanosome Morphology and Inferred Original Chemistry. The fossils in our analyses include amphibians, birds, mammals, fish, and cephalopods that preserve putative melanosomes or melanin granules (Fig. 1 and *SI Appendix*, Table S1), and which range in age from Carboniferous (Fig. 1 *G* and *H*) to Miocene (Fig. 1 *U* and *V*). Material from the Eocene Messel Formation is particularly diverse, including frog eyes (Fig. 1 *Q* and *R*) and skin (Fig. 1 *S* and *T*), mammalian hair (two bat species, *Palaeochiropteryx* and *Hassianycteris*) (Fig. 1 *I−L*), and two feathers (Fig. 1 *A, B, E,* and *F*), which serve to test for variation in melanin composition (eumelanin−phaeomelanin) within a single depositional and taphonomic system. We infer that the Messel feathers (Fig. 1 *A, B, E,* and *F*) are iridescent based upon the morphologies of the putative melanosomes, which were analyzed by quadratic discriminant analysis, as previously used by Li et al. (3, 4) for birds. Likewise, we infer that the two bats (Fig. 1 *I−L*) were brown, based upon observations of small (<650 nm), subrounded putative melanosomes, suggesting a predominantly phaeomelanin-based composition.

TOF-SIMS and PCA. Overall, the mass spectra of the fossils qualitatively resemble those observed in previous studies (7, 8) relative to extant melanin reference samples herein (nine bird species, frogs, and a cephalopod ink) and our chosen negative control samples
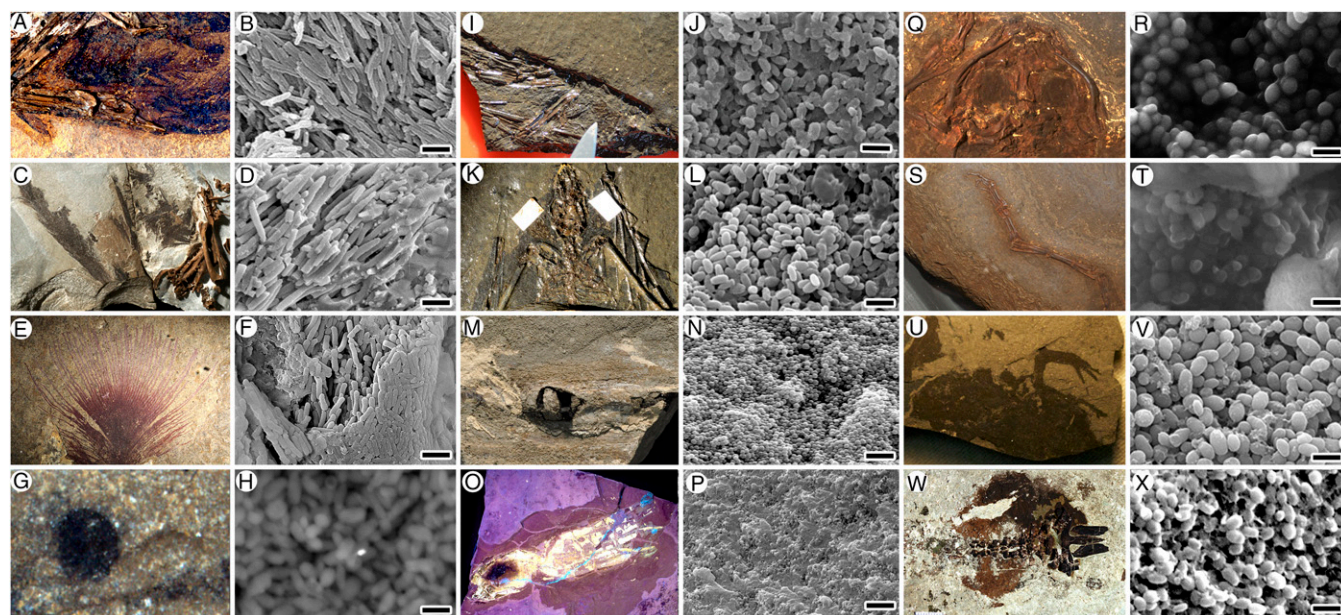
Fig. 1. Range of fossils analyzed with TOF-SIMS imaged using photography and under SEM. (*A* and *B*) Fossil complete bird with associated feathers, *Messelornis*, Messel, Eocene, Germany. (*C* and *D*) Articulated bird associated with feathers, undescribed, Fur Formation, Eocene, Denmark. (*E* and *F*) Isolated feather previously described as iridescent (2), Messel, Eocene, Germany. (*G* and *H*) Complete cyclostome fish preserving the eye, detailed, Mazon Creek, Carboniferous. (*I* and *J*) The bat *Hassianycteris*, Messel, Eocene, Germany. (*K* and *L*) The bat *Palaeochiropteryx*, Messel, Eocene, Germany. (*M* and *N*) Fossil ink sac, Lyme Regis, Lower Jurassic, England. (*O* and *P*) Fossil octopus (?*Keuppia*) associated with ink sac, Cretaceous, Hakel, Lebanon; UV image courtesy of Jonathan Jackson. (*Q* and *R*) Fossil frog preserving eyes, *Paleobatrachus*, Messel, Eocene, Germany. (*S* and *T*) Same frog as in *Q*, detailing skin preserved on the hind leg, Messel, Eocene, Germany. (*U* and *V*) Fossil frog, Pipidae, Mush Valley, Miocene, Ethiopia. (*W* and *X*) Fossil tadpole, *Pelobates*, Oligocene, Enspel, Germany. Specimens were photographed under normal light, except in *O*, which is imaged under UV light as well as scanning electron microscopy images. See *SI Appendix*, Table S1, for details. (Scale bars, 1 µm.)
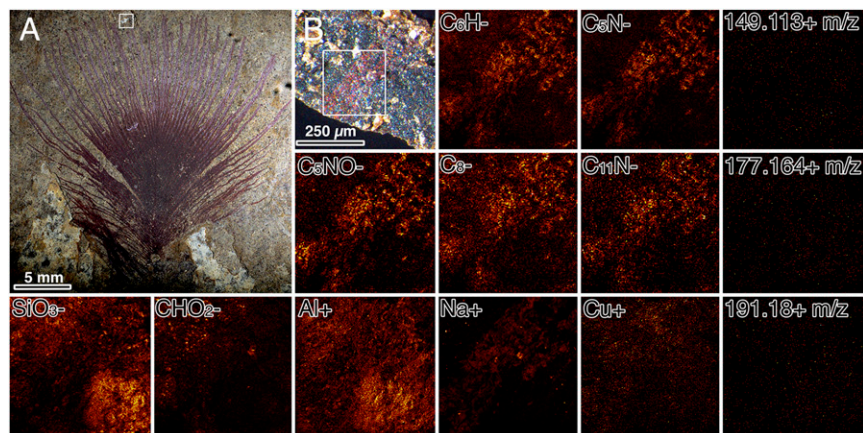
Fig. 2. TOF-SIMS intensity maps of selected positive and negative secondary ions from an Eocene iridescent feather, SMF-ME 3850 from Messel, Germany. (*A*) Entire feather imaged under normal light. (*B*) Microscopic image of sample analyzed under TOF-SIMS. TOF-SIMS intensity distributions are labeled by the predicted secondary ion. Note the correlation of secondary ions, previously noted in melanins (7) in the feather barb relative to the matrix, whereas SiO_3-, $Al+$, and CHO_2- are more intense in the matrix, which can be attributed to the presence of aluminosilicates, whereas the presence of CHO_2- could be due to other organic-rich sources, such as algae or pollen. Sodium ($Na+$) is localized to the feather, whereas the presence of copper ($Cu+$) shows no particular correlation to the feather imprint. Bacterial biomarkers for hopanoids were also mapped: $m/z = 149.113+$, $m/z = 177.164+$, and $m/z = 191.18+$. These did not exhibit any particular localization, or any significant quantity in the spectra obtained.

(fossilized and modern leaves, fossil organic sediment matrix samples, carbon tape used in SEM, and bakers yeast). In some fossil samples, we note the presence of other inorganic and organic secondary ions (*SI Appendix*, Fig. S2) in addition to the melanin characteristic peaks. The patterns of secondary ions previously listed for eumelanin present in the fossil organic imprints (7) were distinct relative to the matrix. In an iridescent feather, previously described (2, 31), we mapped an isolated barb and barbules plus the associated sediment (Fig. 2). The secondary ions previously selected as markers for eumelanin were indeed highly expressed in the feather, but to some extent also in the adjacent matrix. Generally, C_nH- fragments are less specific than C_nN-. The lack of specificity of such organic fragments demonstrates the need to evaluate the spectrum objectively, rather than by eye (7, 8), to diagnose the presence and the state of putative melanin in these fossils. The adjacent matrix exhibited strong signals for inorganic secondary ions, such as SiO_3- and $Al+$, (Fig. 2), which indicate the presence of clay

minerals, whereas the presence of CO_2H- localized in small rounded clusters at one side of the matrix (upper left side of the mapped region) might represent the remains of organic microfossils potentially rich in carboxyl groups (Fig. 2). To investigate the distribution of bacterially derived biomarkers, we chose three m/z positive ions, diagnostic for hopanoids ($m/z = 149.113$, 177.164, 191.18) (32–34). None was present in noticeable quantities or concentrated in either the feather or the matrix (Fig. 2).

As in previous TOF-SIMS studies of fossil melanin (8), the spectra obtained from extant (see *SI Appendix*, Fig. S2 *E and F*) and fossil melanosomes (see *SI Appendix*, Fig. S2 *A–D*) can be differentiated by analyzing the characteristic melanin peaks using PCA (Fig. 3). In our PCA analysis (Fig. 3*A*), freshly extracted melanin plots in a region distinct from fossil samples, whereas the matured samples plot in an intermediate region. Modern samples exposed to higher temperatures generally fall closer to fossil samples along the PC1 axis. Within each sample category
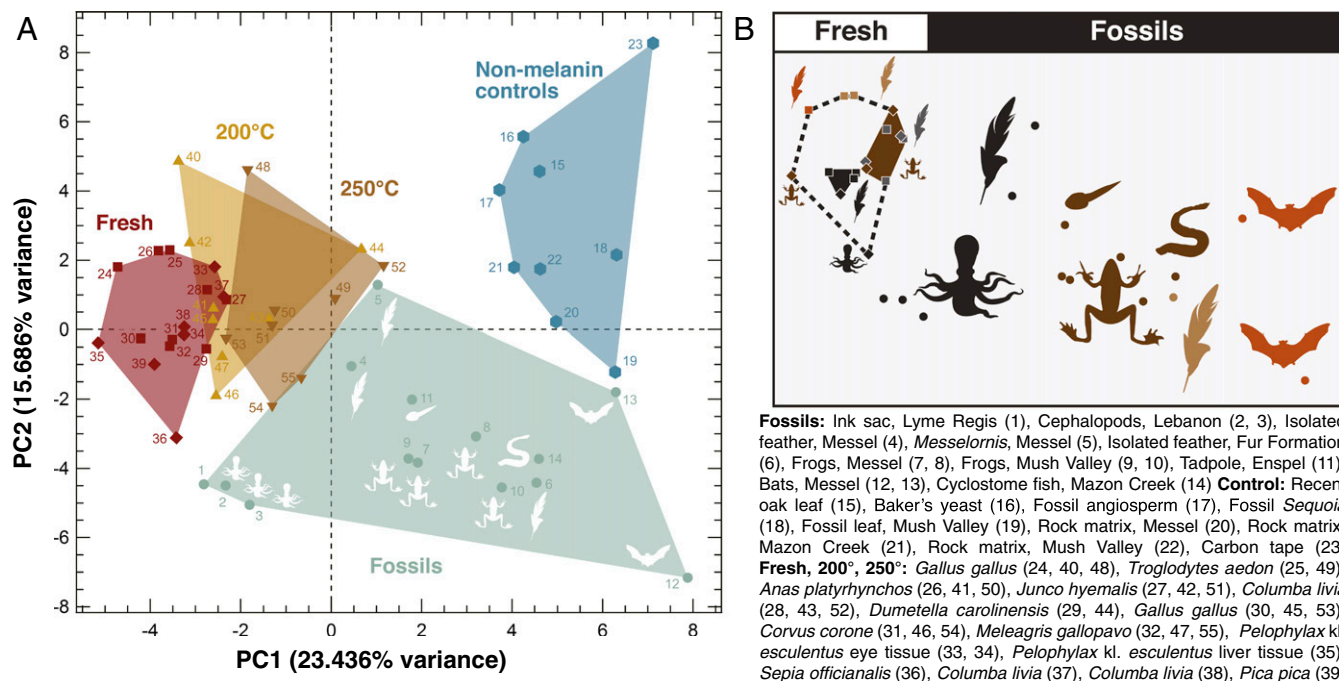

Fig. 3. PCA of fossil melanin TOF-SIMS spectra and comparative samples. (*A*) Principal component plot of TOF-SIMS spectra with the area defined by each sample category (fresh, fossil, matured 200 °C/250 bar, 250 °C/250 bar) indicated with distinct color. (*B*) Schematic overview of distribution of samples according to inferred/observed color/taxonomy. For loadings, see *SI Appendix*, Fig. S4.

Fossils: Ink sac, Lyme Regis (1), Cephalopods, Lebanon (2, 3), Isolated feather, Messel (4), *Messelornis*, Messel (5), Isolated feather, Fur Formation (6), Frogs, Messel (7, 8), Frogs, Mush Valley (9, 10), Tadpole, Enspel (11), Bats, Messel (12, 13), Cyclostome fish, Mazon Creek (14) **Control:** Recent oak leaf (15), Baker's yeast (16), Fossil angiosperm (17), Fossil *Sequoia* (18), Fossil leaf, Mush Valley (19), Rock matrix, Messel (20), Rock matrix, Mazon Creek (21), Rock matrix, Mush Valley (22), Carbon tape (23) **Fresh, 200°, 250°:** *Gallus gallus* (24, 40, 48), *Troglodytes aedon* (25, 49), *Anas platyrhynchos* (26, 41, 50), *Junco hyemalis* (27, 42, 51), *Columba livia* (28, 43, 52), *Dumetella carolinensis* (29, 44), *Gallus gallus* (30, 45, 53), *Corvus corone* (31, 46, 54), *Meleagris gallopavo* (32, 47, 55), *Pelophylax* kl. *esculentus* eye tissue (33, 34), *Pelophylax* kl. *esculentus* liver tissue (35), *Sepia officinalis* (36), *Columba livia* (37), *Columba livia* (38), *Pica pica* (39)

(fresh, 200 °C/250 bar, 200 °C/250 bar), eumelanin- and phaeo-melanin-rich samples separate along the PC2 axis (Fig. 3 A and B). The fossil melanin samples show a trend in which the squid ink (Jurassic, Cretaceous) and the two iridescent feathers (iridescence is generated by eumelanosomes) from Messel plot on one end of the PC1 axis, whereas the presumed brown (phaeomelanin-rich) bat samples, also from Messel, plot opposite. Amphibians (skin and eyes, Eocene–Miocene, including Messel), the feather from Eocene of the Fur Fm., and the Carboniferous fish eye plot in intermediate positions (Fig. 3). No clear trend can be attributed to geologic age or burial history of the samples, but there is distinct clustering by phylogeny and presumed original melanin composition as inferred from melanosome morphology (Fig. 3B).

The chemical distinction between phaeomelanin-rich and eumelanin-rich melanosomes of both the fresh and matured feathers sorts along the PC2 axis. The fossil samples inferred to consist of eumelanin and phaeomelanin spread along the PC1 axis rather than the PC2 axis. Nevertheless, they have a similar trend in taxonomic distribution: Squid ink and iridescent feathers plot at one end, and putative phaeomelanin-rich melansomes from the fossil bats plot at the other, with amphibians in between. It appears, from the maturation experiments, that the variations in eumelanin and phaeomelanin experience a clockwise rotation in the spread of the spectra in the PCA plot, an observation deserving further scrutiny.

We further notice a distinct trend in the melanin TOF-SIMS spectra when comparing the maturation experiments to the fresh samples. The relative intensity of peaks within the spectrum is more attenuated in the matured samples (see *SI Appendix*, Fig. S1) compared with the fresh ones (the differences between strong and weak peaks are greater). A similar trend is observed in fossil samples and can probably be ascribed to the loss of smaller, volatile compounds, such as NH_4, H_2O, and CO_2, by dehydration of the melanin (35).

Melanosome Shrinkage During Burial Diagenesis and Maturation Experiments. Previous maturation experiments suggest melanosomes shrink up to 20% when exposed to temperatures and pressures simulating diagenesis (19). In melanosomes extracted from the black feather of a crow, *Corvus* (Fig. 4D), we observed no more than 10% shrinkage. Fossil melanosome impressions in rock matrix can be larger than three-dimensionally preserved melanosomes (5, 18), directly demonstrating that melanosomes undergo shrinkage during diagenesis. The shrinkage is most likely due to the aforementioned loss of volatiles through dehydration (35). In our experiments, both eumelanin and phaeomelanin released volatile compounds with distinct odors (e.g., phaeomelanin had a characteristic sulfuric smell, and eumelanin smelled like "old cigar"), suggesting alterations of their molecular composition. Artificially matured melanosomes are occasionally altered beyond recognition (Fig. 4). Where original morphology is distinguishable, the melanosomes can be broken, thus affecting precise measurements of melanosome dimensions (Fig. 4D; see *SI Appendix*, Fig. S3). Two experimental gold tubes ruptured during the experiment, and water entered the tube. The melanosomes in these samples merged completely (Fig. 4 A and E, *Middle*). Such merged textures resemble conditions seen in highly altered fossils, such as the isolated feather of *Archaeopteryx* (5), as well as some Jehol and Green River fossils. Maturation experiments are an accelerated approximation of diagenetic conditions, which take place under lower temperature/pressure regimes over millions of years. Such experiments can yield textures markedly different from those observed in fossils (29); therefore, caution should be exercised when using high-temperature maturation experiments for making predictions regarding the alteration of fossil tissues (19). However, the fact that the transformation of the matured melanin to solid organic material does not seem to affect the chemical spectra in a noticeable way suggests that melanin can be identified in highly altered fossils.
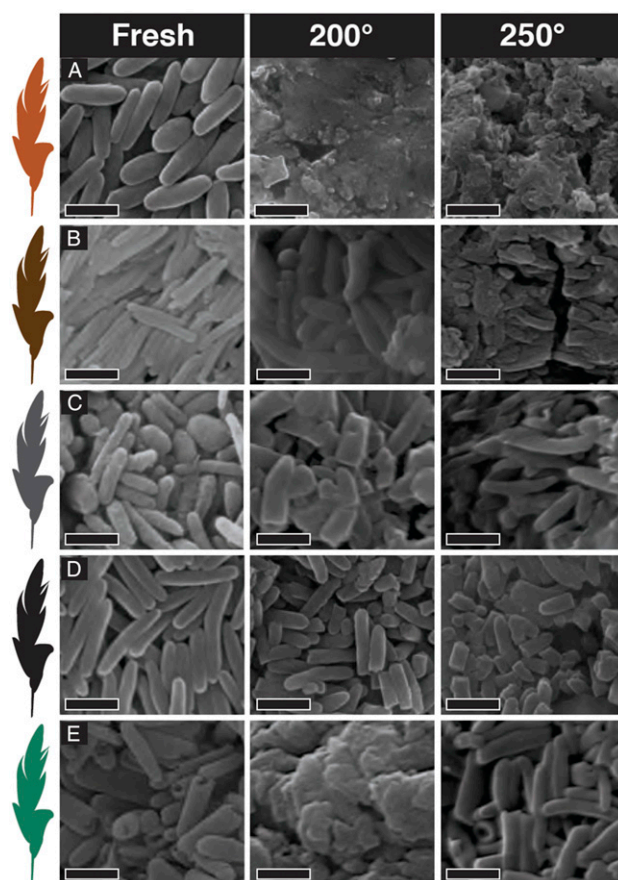

Fig. 4. Scanning electron images of experimentally matured melanosomes. (*A*) *Gallus gallus* feather (red/brown). (*B*) *Troglodytes aedon* feather (brown). (*C*) *Junco hyemalis* feather (gray). (*D*) *Corvus corone* feather (black). (*E*) *Meleagris gallopavo* feather (iridescent). (Scale bar, 1 μm.)

Discussion

TOF-SIMS, as a minimally destructive tool capable of in situ molecular analyses, has exceptional promise in analyzing biomolecule preservation in rare fossils. By combining SEM imaging and TOF-SIMS experiments, we demonstrate that the organic residues in a diverse sample of vertebrates and cephalopods are consistent with the hypothesis that they comprise fossilized, altered melanin. These observations corroborate the hypothesis that the oblong and spheroidal microbodies in these carbonaceous compressions are indeed melanin-bearing melanosomes (1) rather than bacteria (10, 11, 36). A recent review argued that the ubiquity of bacteria, their supposed propensity to fossilize, and their similarity in size and scale to melanosome microbodies (36) cast doubt on morphology-based identification of fossil melanosomes. However, our broad survey of organic microbodies in fossil animal tissues demonstrates that morphology and arrangement can be used with confidence to identify candidate fossil melanosome microbodies. Organic material is often lost due to oxygenated meteoric weathering, which complicates melanin detection. But melanosome impressions are often preserved, showing similar morphology and arrangement to extant counterparts, whereas bacterial communities exhibit a much broader range of morphologies. Such impressions are not seen randomly on fossils or rock surfaces other than original melanin-bearing tissues, which goes to show that the ubiquitous bacteria are unlikely to be responsible for them, even occasionally. Even though rich bacterial flora would have been implicated in the life, death, and decay of these tissues, it is not fossilized as

organic microbodies except when encapsulated in cherts. Archaea has never been found fossilized, yet its biomarkers are ubiquitous (35). Although bacterial activity are relevant in other aspects of soft tissue fossilization, such as in pyrite (23) and calcium phosphate (23, 24) mineralization, the latter of which appears to occasionally preserve microbial fabrics and potentially also bacterial microbodies, the suggestion (36) that bacteria only fossilize locally in melanin-bearing tissues, to the exclusion of other, more decay-prone tissues, is untenable. In fact, the argument could be considered *reductio ad absurdum*, the predictions of which are effectively falsified by the results of our experiments and previous work demonstrating the unique arrangement of melanosomes in pigmented and iridescent feathers, which bacteria would not replicate (1, 2).

Glass et al. (25, 27) documented, using pyrolysis GC-MS, that Jurassic cephalopod ink melanin produced sulfur-containing compounds, such as thiophenes and alkylated thiophenes, which are not expected phaeomelanin products. This suggests a role for early diagenetic alteration and preservation reactions in euxinic (sulfidic) environments, which essentially vulcanize organic substances. It could be surmised that these reactions mainly affect marine fossils due to the higher sulfate content of marine settings. We note, however, that feathers and hair from the freshwater locality, Messel oil shale, are locally enriched in pyrite framboids, which suggests availability of reactive hydrogen sulfide, as confirmed by other studies (38). A more pressing concern is that the data from the TOF-SIMS analyses used in melanin characterization (7, 8) are based on assemblages of fragment ions from larger molecules. Individually, these small fragments have little diagnostic value and could potentially lead to conflation of original sulfur-containing melanin (phaeomelanin) and the products of secondarily sulfurized (eu)melanin. However, the apparent grouping of fossil melanosomes by taxonomy and chemistry, rather than by environmental setting, suggests that diagenetic sulfur incorporation, if it occurs, is negligible.

In addition, we document the presence of melanosomes in fossil mammals for the first time, to our knowledge, both chemically and morphologically, showing that two species of bats from the Eocene of Messel (48.2 Ma) were originally brown. Amphibian melanosomes are intermediate in morphology between eumelanosomes and phaeomelanosomes (Fig. 1 *Q−Y*). These results contradict recent studies arguing that melanosomes outside of paravian dinosaurs (including birds) and mammals lack morphological distinction (13), and that they can reflect differences in physiology. Rather, amphibian melanosomes are generally of mixed composition, and thus intermediate in morphology. The fossil Carboniferous fish shows a similar trend in our PCA plot, also suggesting a mixed melanin composition. Another study used pyrolysis GC-MS to study a fossil tadpole from Enspel (38) and could not conclusively present evidence for melanin due to lack of comparisons to extant, fossil, or artificially matured melanin samples and to previous studies on fossil eumelanin using the same experimentation (25, 27). However, we show here that, in our comparative framework, the Enspel melanosomes do retain melanin residues, contrary to earlier studies suggesting a microbial origin (39).

The emerging picture, suggesting a more widespread occurrence of phaeomelanin in groups other than mammals and birds, is of interest. Phaeomelanin was thought to be restricted to warm-blooded animals, presumably evolving convergently for metabolic reasons (40). However, it appears that phaeomelanin is actually more widespread in ectothermic organisms than previously thought (14–17). As proposed recently (20), the more pure melanins in mammals and birds could reflect the marked shift in external integument with the evolution of hair and feathers for insulation in these warm-blooded animals rather than physiology (13). With the evolution of insulating features covering the body, more-colorful chromatophores were lost,

and selection pressure to evolve more-radical variants of melanins to provide diverse colors, iridescence, and patterns came into play.

Despite the advances in the identification of melanin by mass spectrometric methods, confident reconstruction of ancient color relies on a combination of both chemical analyses and interpretations of fossil melanosome morphology. Maturation experiments confirm the presence of diagenetically altered melanin by reconstructing the diagenetic pathways that lead to fossil melanin. Furthermore, we show here that TOF-SIMS is able to distinguish between different mixtures of eumelanin and phaeomelanin, which are congruent with the observed melanosome morphology. Electron microscopy is still necessary for inferring ancient melanin-based color patterns (1), as melanosome chemistry does not distinguish gray from brown colors (Fig. 3*B*), the relative brightness of a color pattern, or the propensity for melanosomes to form iridescent nanostructures. It is necessary to do a detailed taphonomic study of each case to understand the degree of alteration and shrinkage of the melanosomes within the fossil (20). Statistical quadratic discriminant analyses of melanosome morphology allow for inferring melanin-based colors (black, brown, gray) and iridescence in birds with high accuracy (3, 4). Relative brightness can be assessed through the characterization of melanosome density (6).

Materials and Methods

Specimens. For details on specimens, see *SI Appendix*, Table S1.

Melanin Extractions. A modified protocol (41) for enzyme melanin extraction was used to obtain purified melanin samples from a variety of tissues. Bird samples used in maturation experiments were similar taxonomically to those published recently (42). Additional samples (100–500 mg) were washed three times with 1 mL acetone and once with biomolecular grade water. They were then added to 1.5 mL of phosphate buffer and DTT. Samples were then incubated for 24 h at 37.5 °C and stirred at 200 rpm. Then, 1.5 mL phosphate buffer (15 mL), DTT (5 μL), and Proteinase-K (5 mg) were added, and the samples were again incubated for 24 h at the same temperature and speed. The samples were removed and centrifuged for 3 min at 16.1 relative centrifugal force before the pellets were washed in biomolecular-grade water six times. Then, 1.5 mL of phosphate buffer (15 mL), DTT (15 μL), and Papain (5 mg) were added to each sample, and samples were incubated for 24 h. Samples were then washed six times with biomolecular-grade water; 1.5 mL of phosphate buffer, DTT, and Proteinase-K were added in the same quantities as before, and samples were incubated for 24 h. Triton X-100 (0.05 mL/1 mL) was added, and samples were stirred for 4 h. Samples were then washed nine times with biomolecular-grade water, and 1.5 mL of phosphate buffer, DTT, and Proteinase-K were added before they were incubated for 24 h. Samples were washed with acetone and washed six times with biomolecular-grade water. Then, 1.5 mL of phosphate buffer, DTT, and Proteinase-K were added, and the samples were incubated for 24 h. This step was repeated for three additional days for tissue samples. On the final day, specimens were washed three times with biomolecular-grade water and left to dry for 1 h under a laminar flow hood.

Maturation Experiments. We performed 20 maturation experiments on feathers of nine species of birds, based on a protocol recently used in the analysis of morphological changes in melanosomes (19). A portion of the melanosome extract was left unaltered for analysis of fresh melanin. Each experiment consisted of 1.0–6.6 mg of feather, weighed into 3-mm-o.d. gold capsules that had been welded closed at one end using an oxyacetylene torch, and then each capsule was welded shut at the other end. Each capsule was then placed inside a Ni alloy pressure vessel, along with a Ni filler rod, and pressurized with water to 25 MPa. Each pressure vessel was then placed inside a furnace and heated to either 200 °C or 250 °C, and held at 25 MPa and temperature for 24 h. Pressure was measured to ±0.1 MPa; the K-type thermocouples used have been found to be precise to ±5 °C. The use of the Ni rod fixed the oxygen fugacity at about Ni–NiO. The experiment was quenched after 24 h by removing the pressure vessel from the furnace and, first, blowing on the vessel with compressed air for about 30 s, and then immersing it into a water bath. All capsules were removed from their pressure vessels and weighed to check that no leaks occurred during the experiment. The capsules were then cracked open, and the samples were extracted and mounted on SEM stubs for TOF-SIMS analysis and SEM analysis.

TOF-SIMS and PCA. An ION-TOF TOF-SIMS.5 was used with a pulsed (18 ns, 10 kHz) analysis ion beam consisting of Bi_3^+ clusters at 30-kV ion energy, which was raster-scanned over areas that typically varied between $100 \times 100 \ \mu m^2$ and $500 \times 500 \ \mu m^2$, depending on the quality (i.e., corrugation and conductivity) of the sample surface. The polyatomic sputtering was selected to further enhance the signal and reduce fragmentation of large organic molecules (43–45). To reduce the sputtering-induced sample charging, a constant energy (21 eV) electron beam was shot on the sample during the data acquisition. All detected secondary ions had negative polarity and an average mass resolution of ∼1–3,000 (m/δm). The base pressure during acquisition was $<1 \times 10^{-8}$ mbar. In addition, we used the Burst Alignment mode on one sample (SMF ME 3850) to create high lateral resolution maps of the species of interest. (Fig. 2). Some samples were coated with gold (Au) before analysis, which does not seem to affect our results. Mass calibration was performed by identifying the following carbon cluster peaks: C−, C_2−, C_3−, C_4−, C_5−, C_6−, C_7−, C_8−, and C_9−. In some spectra, some of these peaks were difficult to identify and thus not chosen. Appropriate regions of interest were selected from the initially acquired data to ensure that the mass spectra were representative for the samples under investigation and to minimize effects of topography. Following previous work (8), 55 melanin characteristic peaks were analyzed for each sample, and PCA (Fig. 3 and SI Appendix, Fig. S4) was performed on the ensemble to determine the correlations between samples. To give each peak the same weight in the PCA, the peak intensity of a certain mass was normalized to the standard deviation of all peak intensities of the same mass from all samples entering the analysis.

1. Vinther J, Briggs DEG, Prum RO, Saranathan V (2008) The colour of fossil feathers. *Biol Lett* 4(5):522–525.
2. Vinther J, Briggs DEG, Clarke J, Mayr G, Prum RO (2010) Structural coloration in a fossil feather. *Biol Lett* 6(1):128–131.
3. Li Q, et al. (2010) Plumage color patterns of an extinct dinosaur. *Science* 327(5971):1369–1372.
4. Li Q, et al. (2012) Reconstruction of *Microraptor* and the evolution of iridescent plumage. *Science* 335(6073):1215–1219.
5. Carney RM, Vinther J, Shawkey MD, D'Alba L, Ackermann J (2012) New evidence on the colour and nature of the isolated *Archaeopteryx* feather. *Nat Commun* 3:637.
6. Field DJ, et al. (2013) Melanin concentration gradients in modern and fossil feathers. *PLoS One* 8(3):e59451.
7. Lindgren J, et al. (2012) Molecular preservation of the pigment melanin in fossil melanosomes. *Nat Commun* 3:824.
8. Lindgren J, et al. (2014) Skin pigmentation provides evidence of convergent melanism in extinct marine reptiles. *Nature* 506(7489):484–488.
9. Mcnamara ME, Orr PJ (2008) Experimental degradation of vertebrates: Taphonomy of keratinous tissues and implications for the fossil record. *Palaeontol Assoc Newsl* 69:29.
10. Moyer AE, et al. (2014) Melanosomes or microbes: testing an alternative hypothesis for the origin of microbodies in fossil feathers. *Sci Rep* 4:4233.
11. Mcnamara ME, et al. (2010) Exceptionally preserved tadpoles from the Miocene of Libros, Spain: Ecomorphological reconstruction and the impact of ontogeny upon taphonomy. *Lethaia* 43(3):290–306.
12. Wakamatsu K, Ito S (2002) Advanced chemical methods in melanin determination. *Pigment Cell Res* 15(3):174–183.
13. Li Q, et al. (2014) Melanosome evolution indicates a key physiological shift within feathered dinosaurs. *Nature* 507(7492):350–353.
14. Roulin A, Mafli A, Wakamatsu K (2013) Reptiles produce pheomelanin: Evidence in the eastern Hermann's tortoise (*Eurotestudo boettgeri*). *J Herpetol* 47(2):258–261.
15. Wolnicka-Glubisz A, Pecio A, Podkowa D, Kolodziejczyk LM, Plonka PM (2012) Pheomelanin in the skin of *Hymenochirus boettgeri* (Amphibia: Anura: Pipidae). *Exp Dermatol* 21(7):537–540.
16. Kottler VA, Künstner A, Schartl M (2015) Pheomelanin in fish? *Pigment Cell Melanoma Res* 28(3):355–356.
17. Speiser DI, DeMartini DG, Oakley TH (2014) The shell-eyes of the chiton *Acanthopleura granulata* (Mollusca, Polyplacophora) use pheomelanin as a screening pigment. *J Nat Hist* 48(45-48):2899–2911.
18. Clarke JA, et al. (2010) Fossil evidence for evolution of the shape and color of penguin feathers. *Science* 330(6006):954–957.
19. McNamara ME, Briggs DE, Orr PJ, Field DJ, Wang Z (2013) Experimental maturation of feathers: Implications for reconstructions of fossil feather colour. *Biol Lett* 9(3):20130184.
20. Vinther J (2015) A guide to the field of palaeo colour: Melanin and other pigments can fossilise: Reconstructing colour patterns from ancient organisms can give new insights to ecology and behaviour. *BioEssays* 37(6):643–656.
21. Gehling JG (1999) Microbial mats in terminal Proterozoic siliciclastics: Ediacaran death masks. *Palaios* 14(1):40–57.
22. Westall F (1999) The nature of fossil bacteria: A guide to the search for extraterrestrial life. *J Geophys Res* 104(E7):16437–16451.
23. Briggs DEG (2003) The role of decay and mineralization in the preservation of soft-bodied fossils. *Annu Rev Earth Planet Sci* 31:275–301.
24. Muscente A, Hawkins AD, Xiao S (2015) Fossil preservation through phosphatization and silicification in the Ediacaran Doushantuo Formation (South China): A comparative synthesis. *Palaeogeogr Palaeoclimatol Palaeoecol* 434:46–62.
25. Glass K, et al. (2012) Direct chemical evidence for eumelanin pigment from the Jurassic period. *Proc Natl Acad Sci USA* 109(26):10218–10223.
26. Tanaka G, et al. (2014) Mineralized rods and cones suggest colour vision in a 300 Myr-old fossil fish. *Nat Commun* 5:5920.
27. Glass K, et al. (2013) Impact of diagenesis and maturation on the survival of eumelanin in the fossil record. *Org Geochem* 64:29–37.
28. Greenwalt DE, Goreva YS, Siljeström SM, Rose T, Harbach RE (2013) Hemoglobin-derived porphyrins preserved in a Middle Eocene blood-engorged mosquito. *Proc Natl Acad Sci USA* 110(46):18496–18500.
29. Stankiewicz B, et al. (2000) Alternative origin of aliphatic polymer in kerogen. *Geology* 28(6):559–562.
30. Gupta NS, Michels R, Briggs DEG, Evershed RP, Pancost RD (2006) The organic preservation of fossil arthropods: An experimental study. *Proc Biol Sci* 273(1602):2777–2783.
31. Vitek NS, Vinther J, Schiffbauer JD, Briggs DE, Prum RO (2013) Exceptional three-dimensional preservation and coloration of an originally iridescent fossil feather from the Middle Eocene Messel Oil Shale. *Palaeontol Z* 87(4):493–503.
32. Steele A, Toporski J, Avci R, Guidry S, McKay D (2001) Time of flight secondary ion mass spectrometry (ToFSIMS) of a number of hopanoids. *Org Geochem* 32(7):905–911.
33. Siljeström S, et al. (2009) Detection of organic biomarkers in crude oils using ToF-SIMS. *Org Geochem* 40(1):135–143.
34. Leefmann T, et al. (2013) Spectral characterization of ten cyclic lipids using time-of-flight secondary ion mass spectrometry. *Rapid Commun Mass Spectrom* 27(5):565–581.
35. Briggs DE, Summons RE (2014) Ancient biomolecules: Their origins, fossilization, and role in revealing the history of life. *BioEssays* 36(5):482–490.
36. Lindgren J, et al. (2015) Interpreting melanin-based coloration through deep time: a critical review. *Proc R Soc B* 282(1813):20150614.
37. Bauersachs T, Schouten S, Schwark L (2014) Characterization of the sedimentary organic matter preserved in Messel oil shale by bulk geochemistry and stable isotopes. *Palaeogeogr, Palaeoclimatol, Palaeoecol* 410:390–400.
38. Barden HE, et al. (2015) Bacteria or melanosomes? A geochemical analysis of microbodies on a tadpole from the Oligocene Enspel Formation of Germany. *Palaeobio Palaeoenv* 95(1):33–45.
39. Toporski J, et al. (2002) Morphologic and spectral investigation of exceptionally well-preserved bacterial biofilms from the Oligocene Enspel formation, Germany. *Geochim Cosmochim Acta* 66(10):1773–1791.
40. Galván I, Ghanem G, Møller AP (2012) Has removal of excess cysteine led to the evolution of pheomelanin? Pheomelanogenesis as an excretory mechanism for cysteine. *BioEssays* 34(7):565–568.
41. Liu Y, et al. (2003) Comparison of the structural and physical properties of human hair eumelanin following enzymatic or acid/base extraction. *Pigment Cell Res* 16(4):355–365.
42. Liu SY, Shawkey MD, Parkinson D, Troy TP, Ahmed M (2014) Elucidation of the chemical composition of avian melanin. *RSC Adv* 4(76):40396–40399.
43. Zimmerman JD, et al. (2013) Control of interface order by inverse quasi-epitaxial growth of squaraine/fullerene thin film photovoltaics. *ACS Nano* 7(10):9268–9275.
44. Sai N, et al. (2012) Understanding the interface dipole of copper phthalocyanine (CuPc)/C60: Theory and experiment. *J Phys Chem Lett* 3(16):2173–2177.
45. Chou H, Ismach A, Ghosh R, Ruoff RS, Dolocan A (2015) Revealing the planar chemistry of two-dimensional heterostructures at the atomic level. *Nat Commun* 6:7482.

EARTH, ATMOSPHERIC, AND PLANETARY SCIENCES

EVOLUTION